J. Am. Soc. Mass Spectrom. (2014) 25:1253–1262
DOI: 10.1007/s13361-014-0893-0

RESEARCH ARTICLE

Detailed Study of Cyanobacterial Microcystins Using High Performance Tandem Mass Spectrometry

Yulin Qi, Stella Bortoli, Dietrich A. Volmer

Institute of Bioanalytical Chemistry, Saarland University, Campus B2.2, 66123 Saarbrücken, Germany

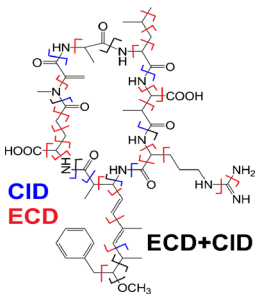

Abstract. Microcystins (MC) are a large group of toxic cyclic peptides, produced by cyanobacteria in eutrophic water systems. Identification of MC variants mostly relies on liquid chromatography (LC) combined with collision-induced dissociation (CID) mass spectrometry. Deviations from the essential amino acid complement are a common feature of these natural products, which makes the CID analysis more difficult and not always successful. Here, both CID and electron capture dissociation (ECD) were applied in combination with ultra-high resolution Fourier transform ion cyclotron resonance mass spectrometry to study a cyanobacteria strain isolated from the Salto Grande Reservoir in Sao Paulo State, Brazil, without prior LC separation. CID was shown to be an effective dissociation technique for quickly identifying the MC variants, even those that have previously been difficult to characterize by CID. Moreover, ECD provided even more detailed and complementary information, which enabled us to precisely locate metal binding sites of MCs for the first time. This additional information will be important for environmental chemists to study MC accumulation and production in ecosystems.

Key words: Cyanobacteria, Microcystins, Structural Elucidation, Metal binding, CID, ECD, FTICR-MS

Received: 12 January 2014/Revised: 12 March 2014/Accepted: 16 March 2014/Published online: 30 April 2014

Introduction

Microcystins (MC) are a group of cyanotoxins produced by different cyanobacterial genera such as *Microcystis*, *Nostoc*, *Anabaena*, *Anabaenopsis*, *Hapalosiphon*, and *Aphanocapsa* [1, 2], which occur naturally in surface waters [3, 4]. Studies of MCs are important because of their harmful impact on wildlife, livestock, and humans after accumulation of the toxins in drinking and recreational waters [5]. MCs contain a cyclic heptapeptide of the general structure cyclo(D-Ala^1-X^2-D-MeAsp^3-Z^4-Adda^5-D-Glu^6-Mdha^7) with variable amino acids *X* and *Z*, where D-MeAsp is D-erythro-β-methyl aspartic acid, Adda is a 20-carbon amino acid of the unusual structure of 2S,3S,8S,9S-3-amino-9-methoxy-2,6,8-trimethyl-10-phenyldeca-4E,6E-dienoic acid, and Mdha is N-methyldehydroalanine [6]. Accordingly, MCs are named by using the single-letter abbreviations of the amino acids present in positions 2 and 4 (e.g., MC-LR; see in Figure 1). Moreover, substitutions of amino acids are designated by the standard abbreviation together with their position number (e.g., [D-Asp^3]MC-LR refers to demethylation at position 3 of MC-LR). Until now, over 90 variants of this molecule have already been described [2, 7, 8]. The most common structural variations occur at positions 2 and 4 with substitutions of different L-amino acids and demethylation at positions 3 and 7 [9]. In other cases, demethylation and acetylation of Adda as well as different special configurations such as (6Z) Adda have been reported [10]. Substitutions of the amino acid D-Ala for D-Ser, D-Leu, or Gly, and methyl-esterification of D-Glu have also been observed [8].

Microcystins are classified as hepatotoxins because of their ability to specifically inhibit protein serine/threonine phosphatases (PP1, PP2A) using the rare amino acid Adda within the molecular structure [11]. Furthermore, the Mdha residue of MCs binds covalently to Tyr272/Cys273 in PP1 or Tyr265/Cys269 in PP2A, providing additional stability for the complex [12, 13]. As result of PP inhibition, there is an increase of phosphorylation of cellular proteins, which is the main cause for changes in the whole cell morphology by cytoskeletal rearrangements. Such cytoskeletal damage results in a disruption of liver cell structure and leads to intrahepatic hemorrhage, hemodynamic shock, and death [6]. Moreover, microcystin-induced hyperphosphorylation is

Electronic supplementary material The online version of this article (doi:10.1007/s13361-014-0893-0) contains supplementary material, which is available to authorized users.

Correspondence to: Dietrich Volmer; *e-mail:* Dietrich.Volmer@mx.uni-saarland.de

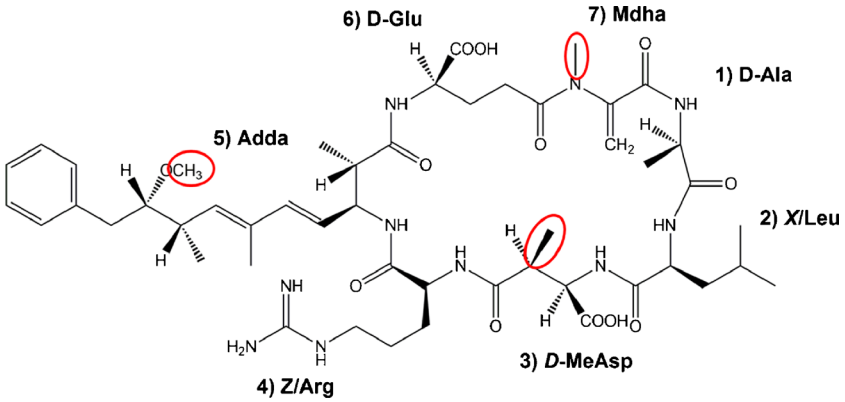

Figure 1. Structure of MC-LR and its possible demethylation sites; the numbering scheme for the amino acids is also shown

the mechanism behind tumor promotion because nodule formation is associated with morphology changes in hepatocytes [5] and because tumor suppressor gene products (retinoblastoma and p53) are both inactivated by phosphorylation [14]. The toxicity of MCs varies from 50 to >1200 $\mu g \cdot kg^{-1}$ (*i.p.* LD_{50} mouse), depending on chemical structure variations. For example, MC-LR and [D-Asp^3] MC-LR show a LD 50*i.p.* in mouse of 50 $\mu g \cdot kg^{-1}$ [15], whereas the toxicity of [Dha^7]MC-LR is 250 $\mu g \cdot kg^{-1}$ [16]. In addition, expression of MCs by alga cells is thought to be regulated by the levels of metal cations taken up from the environment [17, 18], and for this reason, Fe and Cu are used extensively in the control of cyanobacteria genera [19].

The toxicity of these hepatotoxins is as variable as their chemical structures and, therefore, the unequivocal identification of all MC variants produced by individual strains in complex mixtures such as in algal blooms would greatly contribute to an improved risk assessment of their environmental impact. The structural characterization of MCs has been previously achieved by a combination of different analytical techniques, including chiral amino acid analysis, chemical degradation techniques, nuclear magnetic resonance, and mass spectrometry (MS) [10, 20–22]. Currently, liquid chromatography-tandem mass spectrometry (LC-MS/MS) methods are most commonly used to identify MC variants [23–25], with low-energy collision-induced dissociation (CID) being the most common mass spectral technique used for structural elucidation [26–29]. However, conventional low energy CID excites the vibrational modes of the molecules; that is, the weakest bonds are almost always cleaved first during the dissociation process, sometimes after rearrangement reactions [30]. Therefore, even with prior LC separation, unambiguous structural elucidation of MCs has not always been successful [24, 31, 32]. For example, Mayumi et al. were not able to confirm the methylation of Asp or Leu in a MC-LR variant because of the observed lack of cleavage reaction between the two amino acids [31]. Saito et al. failed to determine the metal binding site of MC-LR and MC-RR standards, even by using Fourier transform ion cyclotron resonance mass spectrometry (FTICR-MS) [32].

During last decade, ion-electron dissociation techniques, especially electron capture dissociation (ECD) [33, 34], have been developed that provide complementary structural information to CID. For example, O'Connor and coworkers studied the ECD fragmentation of small, cyclic peptides ($[M+2H]^{2+}$) [35]. In that study, the amino acid losses were unexpected because that they required one electron capture to trigger two or more backbone cleavages. To explain the numerous fragments observed, a radical cascade mechanism was proposed [35]. Chait and coworkers used electron transfer dissociation (ETD) for comprehensive sequence coverage of peptide backbones of cone snail venoms after increasing the charge state of the cysteine-containing peptide toxins [36]. Samgina et al. performed chemical derivatization on the crude secretion of frog species and applied a combination of CID and ECD to successfully identify peptides in the skin secretion of the Caucasian green frog *Rana ridibunda* [37].

Here, both CID and ECD techniques were applied to study the MC variants expressed in a cyanobacterial strain isolated from the Salto Grande Reservoir in Brazil without prior liquid chromatography separation. The MCs of interest were a large group of cyclic peptides with molecular weights around 1000 Da. The complementary information from the two techniques enabled us to unambiguously identify MC variants from cultured cyanobacterial strain samples. Moreover, the metal binding site of MCs was precisely located for the first time; we believe that this discovery will open further avenues for environmental chemists to understand and control the MC production in eutrophic ecosystems.

Experimental

LTPNA 02 Sample

Microcystis aeruginosa LTPNA 02 is a cyanobacterial strain isolated from the Salto Grande Reservoir in Americana, Sao Paulo State, Brazil, and cultivated at the Laboratory of

Toxins and Natural Products of Algae (LTPNA, University of São Paulo, Brazil). The strain was grown in 250 mL flasks for 1 wk as inoculum preparation. The biomass volume was increased by cultivation in 2 L flasks, with 1.6 L of ASM-1 medium [38, 39]. The cultivation took place at 22 $\mu E \cdot m^{-2} \cdot s^{-1}$, 12:12 h (L:D) photoperiod at 25°C (±1°C) with constant aeration for 20 d. The culture was centrifuged at 8000 rpm for 15 min at 4°C and the cell fraction lyophilized. To 50 mg of the lyophilized material, 5 mL of aqueous 90% methanol were added; the mixture was homogenized and submitted to an ultrasonic bath for 15 min, later centrifuged at 10,000 rpm for 10 min at 4°C. The supernatant was filtered using 0.2 µm cellulose acetate filters and diluted 100× with 50:50:1 methanol/water/formic acid mixture.

Microcystin and Metal Complexes

MC-LR and MC-RR standards were purchased from Enzo Life Sciences (Lausen, Switzerland); Fe(II), Fe(III), and Mg sulfate heptahydrates were from Sigma Aldrich (Steinheim, Germany). MC-LR and MC-RR were diluted to 100 µM in methanol to prepare stock solutions. The Mg and Fe complexes were produced by adding their sulfates (1 mM) to the stock solutions. The mixtures were diluted to 0.5 µM with 50:50:1 methanol/water/formic acid solvent prior to mass spectrometry analysis.

FTICR Mass Spectrometry

All samples were ionized using electrospray ionization (ESI) and mass spectra were recorded using a SolariX 7 Tesla FT-ICR mass spectrometer (Bruker Daltonik, Bremen, Germany), equipped with an Infinity cell. For each spectrum, 40–100 individual transients were collected and co-added to enhance S/N [40]. In MS/MS mode, precursor ions were isolated first in the quadrupole and externally accumulated in the hexapole for 0.2–2 s. For CID, 5–20 V collision voltage was applied. For ECD, the accumulated ions were transferred into the ICR cell and irradiated with 1.5 eV electrons from a 1.5 A heated hollow cathode dispenser for 50–200 ms. All spectra were internally calibrated (see peak lists below). Due to H transfer between $c'/z\cdot$ ions in ECD experiments [35, 41, 42], peak assignment was based on matching both the theoretical mass and the isotopic pattern. Either the monoisotopic peak or the most intense peak (if monoisotopic peak was not clearly identifiable) was used for assignment in the peak list.

Results and Discussion

As mentioned in the Introduction, the aim of this study was to elucidate a detailed dissociation scheme for MC compounds using both CID and ECD experiments, with the primary goal of solving two current problems that have been encountered during analysis of these compounds: viz., confident identification of MC variants that exhibit modifications of amino acids in the side chains, and the determination of the exact location of metal binding sites of MCs.

CID and ECD Analysis of Microcystin Variants LR and RR

The primary full scan analysis of the *LTPNA 02* extract showed doubly charged species at *m/z* 498, 491, 520, and 513, which matched the nominal masses of MC-LR, demethyl-MC-LR, MC-RR, and desmethyl-MC-RR, respectively. Therefore, these four species were targeted for further investigation. As the structure of ML-LR (Figure 1) is well established, the species at *m/z* 498 was chosen for investigation first, and the fragmentation techniques CID and ECD were applied to determine its structure, to fully understand the dissociation mechanisms (Figure 2a and b).

The cleavage reactions of MC-LR are illustrated in Figure 2c and d: each arrow represents cleavage of that particular bond; fragment ions are marked by letters. For example, in Table 1 the fragment "bc" at *m/z* 155.0815 indicates the product ion resulting from cleavage of the bonds labeled "b" and "c" in Figure 2c, following the direction of the arrows. As shown, fragmentation by CID was mostly limited to the amide bond plus the classical fragments; that is $[Ph\text{-}CH2\text{-}CHOMe]^+$ (*m/z* 135.0804) from the Adda group in agreement with previous reports [26, 43]. Although most fragments were *b/y* ions, CID fragmentation occurred for all of the seven amino acids within the compound, providing complete sequence of the cyclic peptide. The species at *m/z* 498 from *LTPNA 02* was therefore confirmed to be MC-LR.

In addition to CID, ion-electron fragmentation techniques have proven to be beneficial for structural characterization, as they usually produce extensive and complementary fragmentation for small molecules [44–46]. For this reason, ECD experiments were conducted for MC-LR. As shown in Figure 2b, the intensities of the fragments generated by ECD were much less intense than the precursor ion compared with CID, due to the low electron capture efficiency of the ions and neutralization of the fragments through interaction with the electrons. However, a much higher number of peaks was observed, which were not restricted to *b/y* cleavages from amide bonds or *c/z* ions from typical ECD cleavages at N–Cα bonds. This observed phenomenon can be explained by the "radical cascade mechanism" [35]: the nonergodic cleavage of a cyclic peptide generates a distonic ion and the radical site can propagate along the peptide backbone, causing both secondary backbone and additional side-chain cleavages. Although the ECD spectra appeared more complicated, high performance FTICR-MS enabled confident assignment of all peaks with relative mass errors well below 0.5 ppm (see Tables 1 and 2 as well as Supplementary Material). All CID fragments were observed by ECD. In addition, extensive side-chain losses were also seen. For

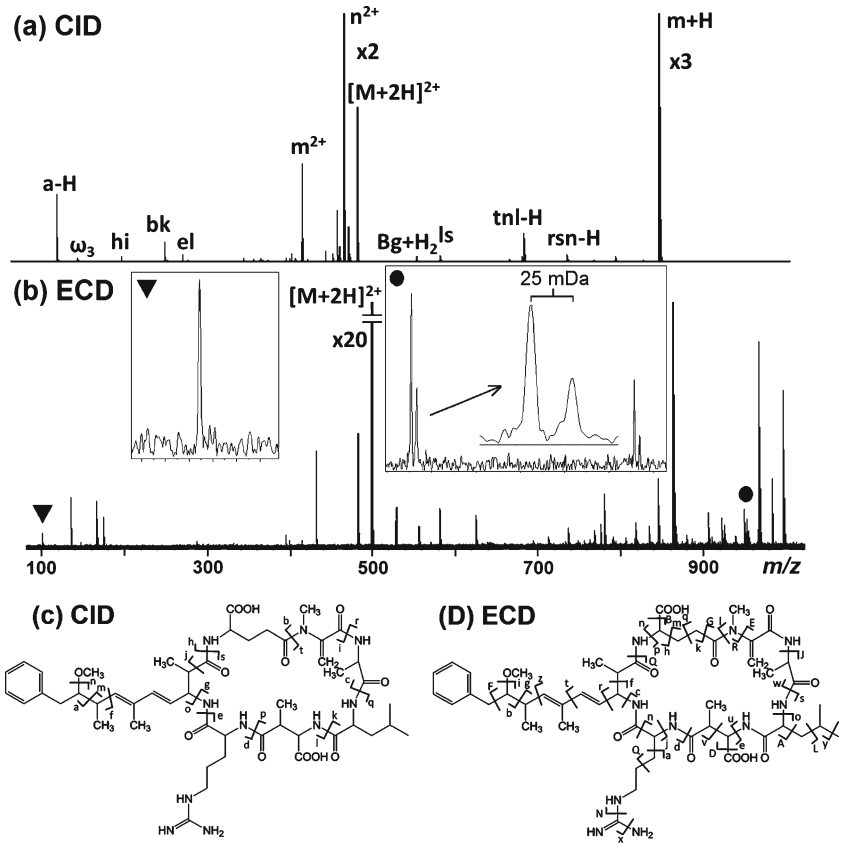

Figure 2. CID (**a**) and ECD (**b**) mass spectra of doubly-charged MC-LR ($[M+2H]^{2+}$, *m/z* 498.28166), with illustration of the fragments assigned from CID (**c**) and ECD (**d**). The insets in (**b**) are x-axis expansions of the peaks corresponding to side chain losses, ▾: $[C_4H_{10}N_3]^+$ from Arg; •:$[C_{48}H_{73}N_8O_{12}]^+$ from Arg and $[C_{46}H_{69}N_{10}O_{12}]^+$ from Leu. The full peak list is available in Tables 1 and 2 (note: peaks used for internal calibration are marked with ▲ in all tables)

example, magnification of a small *m/z* range in Figure 2b revealed two very close isotope patterns ($C_{48}H_{73}N_8O_{12}$ versus $C_{46}H_{69}N_{10}O_{12}$, $\triangle m/z$=25 mDa), resulting from the side chain losses of Arg and Leu, respectively; here, they were well resolved by FTICR-MS. These new fragments from side-chain losses are a very important supplement to the CID data, as this piece of information can provide diagnostic peaks for different peptides, which will be extremely beneficial for identification of the amino acid substitution in unknown MC compounds (see following section). The same experiment was then applied to the species at *m/z* 520; similar cleavages were observed (see Supplementary Material, Figure S1), and thus that species in the *LTPNA 02* extract was identified as MC-RR.

Identifying further Microcystin Variants in LTPNA 02 Extract

The species at *m/z* 491 and 513 in *LTPNA 02* were thought to be the demethylated forms of MC-LR and RR, and they were selected for further analysis. Demethylation of MCs are most commonly observed at positions 3 (substituted by Asp), 7 (by Dha, dehydroalanine), and at the unusual amino acid Adda, which can be substituted by O-demethylAdda (DMAdda) (Figure 1 illustrates these substitutions) [47].

As shown in the previous section, CID generated very simple MS/MS spectra and intensive fragmentations, which makes it a robust method for quickly identifying MCs in complex samples. For this reason, CID was applied to the two species at *m/z* 491 and 513 and the corresponding fragments were assigned. The cleavage map of the *m/z* 491 species (Figure 3a) shows fragments "a" and "r" resulting from the characteristic $[Ph\text{-}CH_2\text{-}CHOMe]^+$ loss of Adda, which clearly indicates that the Adda group remained unchanged in this compound. Detailed interpretation of the spectrum (Supplementary Material, Table S3) revealed that the fragments "bc," "fg," "fc," and "fk" correspond to $[Mdha\text{-}Ala+H]^+$, $[Glu\text{-}Mdha+H]^+$, $[Glu\text{-}Mdha\text{-}Ala+H]^+$, and $[Glu\text{-}Medha\text{-}Ala\text{-}Leu+H]^+$, respectively (Figure 3a). These fragment ions support the presence of a methyl group within the Mdha unit. In addition, the characteristic fragment ions "hi," "hj," "lm," "le," "opn," "oqn," and "lpn" all prove the absence of the methyl group in the MeAsp unit. Therefore, the MC-LR variant found in *LTPNA 02* extracts

Table 1. CID fragments of MC-LR, $[M+2H]^{2+}$ *m/z* 498.28166. Note: peaks used for internal calibration are marked with ▲

Proposed formula	Fragment cleavage	Theoretical *m/z*	Experimental *m/z*	Mass error (ppm)
▲C9H11O	a-H	135.08044	135.08044	0.00
C7H11O2N2	bc	155.08150	155.08151	0.04
C6H13N4O	de	157.10839	157.10838	–0.06
C11H15O	f-H	163.11174	163.11173	–0.07
C6H16N5O	dg+H_2	174.13494	174.13494	0.00
▲C9H13N2O4	hi	213.08698	213.08698	0.00
C10H11N2O5	ij-H_2	239.06625	239.06626	0.05
C13H22N3O3	bk	268.16557	268.16558	0.04
C11H20N5O4	el	286.15098	286.15099	0.03
C11H23N6O4	el+H_2	303.17753	303.17754	0.03
C20H27N2O5	mio-H	375.19145	375.19144	–0.02
C39H56N8O9	$[dni]^{2+}$	390.20796	390.20818	0.55
C18H29N4O6	hk or bp	397.20816	397.20814	–0.05
C17H31N6O5	qe	399.23505	399.23509	0.11
C40H66N10O11	$[m]^{2+}$	431.24508	431.24506	–0.05
C48H72N10O11	$[n]^{2+}$	482.26855	482.26863	0.17
▲C20H39N8O6	rg+H_2	487.29871	487.29869	–0.03
C49H74N10O11	$[M–H_2O]^{2+}$	489.27638	489.27639	0.02
C49H76N10O12	$[M+2H]^{2+}$	498.28166	498.28170	0.08
C24H41N8O7	be	553.30927	553.30929	0.03
C30H43N6O5	nsl-H	567.32895	567.32897	0.04
C24H44N9O7	bg+H_2	570.33582	570.33581	–0.02
C27H44N7O8	tlm+H	594.32459	594.32464	0.09
C31H47N6O6	ls	599.35516	599.35505	–0.18
C31H49N8O9	ilm+H	677.36170	677.36167	–0.05
C29H48N9O10	he	682.35187	682.35185	–0.02
▲C35H50N7O8	tnl-H	696.37154	696.37157	0.05
C36H54N7O9	lt	728.39775	728.39771	–0.06
C39H59N8O7	rsn-H	751.45012	751.45010	–0.03
C39H55N8O9	iln-H	779.40865	779.40883	0.23
C42H60N9O10	cln-H	850.44577	850.44576	–0.01
▲C40H65N10O11	m+H	861.48288	861.48278	–0.11
			Std. Dev.	0.13

was unambiguously identified as [D-Asp^3]MC-LR. By using the same approach, the other species at *m/z* 513 was confirmed to be [D-Asp^3] MC-RR (Figure 3b).

In previous studies, CID analyses have not always unequivocally confirmed the structure of these cyclic peptide compounds, including problems with incomplete peptide sequence ion formation, determination of different methylation sites, and complications from multiple ring openings leading to isobaric linear peptides (i.e., peptides with same masses but varying sequences). For example, a fragment at *m/z* 385 can be assigned as $[Ala\text{-}Adda+H]^+$, $[Leu\text{-}Asp\text{-}Arg+H]^+$, or $[Ala\text{-}Leu\text{-}MeAsp\text{-}Ala+H]^+$, and for this reason, high resolution mass spectrometers such as Orbitrap and FTICR have been applied to the characterization of MCs for unambiguous identification [28, 29, 32, 48]. However, many of these MC molecular or fragment ions are isomers caused by variation or substitution of amino acids (e.g., MeSer/Thr, MeAsp/Glu, Leu/IsoLeu, or peptides contain Mdha-Asp/Dha-MeAsp; MeSer-Asp/Ser-MeAsp), which cannot be distinguished by mass measurement only and, therefore, MS^3 experiments are always required for the MC identification [26, 32, 43, 49]. Here, our CID data (Figure 3) clearly showed that MS^2 was able to achieve full peptide sequence coverage and distinguish the MCs from complex mixtures without prior LC separation. In addition, all *b*/*y* fragments listed in this paper can also be used as diagnostic ions for rapidly identifying MC variants or similar compounds from environmental samples.

Microcystin-Metal Interaction

Although the toxic mechanisms of MCs in humans have been well studied, their biochemistry and behavior in the producing algal cell remains largely unknown. It was found that the production of MCs by cyanobacteria is regulated by metals, which are taken up from the ecosystem [17, 18], and research also suggests that MCs act as intracellular metal transporter in algae because they are not released from the algae until cell death [50].

To help understand the biological function of MCs in cyanobacteria, a useful first step is to study their metal binding complexes. Characterization of the metal binding on MCs has been carried out by polarography [51], UV spectroscopy [52], cyclic and anodic stripping voltammetry [52, 53], and even FTICR-MS [32]. Nevertheless, binding sites remain unidentified because of the weak noncovalent bond formed by the metal. Saito et al. claimed that metal–MC mixtures cannot be observed by ESI and, therefore,

Table 2. ECD fragments of MC-LR, $[M+2H]^{2+}$ *m/z* 498.28166

Proposed formula	Fragment cleavage	Theoretical *m/z*	Experimental *m/z*	Mass error (ppm)
▲C4H10N3	a-H	100.08692	100.08690	–0.20
▲C9H11O	b-H	135.08044	135.08044	0.00
C6H16N5O	cd+H_2	174.13494	174.13494	0.00
C19H32N5O4	efg+H	394.24488	394.24483	–0.13
C23H35N4O2	fj	399.27545	399.27539	–0.15
C19H33N6O4	dhg+H	409.25578	409.25583	0.12
C23H36N5O2	df	414.28635	414.28640	0.12
C40H66N10O11	$[g]^{2+}$	431.24508	431.24518	0.23
C48H72N10O11	$[i]^{2+}$	482.26855	482.26857	0.04
▲C49H76N10O12	$[M+2H]^{2+}$	498.28166	498.28169	0.06
C28H42N5O5	hj	528.31805	528.31809	0.08
C30H46N5O5	jk	556.34935	556.34950	0.27
C24H44N9O7	cl+H_2	570.33582	570.33555	–0.47
C26H45N8O7	mn	581.34057	581.34071	0.24
C27H46N9O8	cm	624.34639	624.34647	0.13
C28H48N9O8	cn-CO_2	638.36204	638.36214	0.16
C34H53N6O6	fo	641.40211	641.40191	–0.31
C30H49N10O9	pqr-H	693.36785	693.36768	–0.25
C37H58N7O7	Qs	712.43922	712.43941	0.27
C33H55N10O9	mpt+H or uvt+H	735.41480	735.41467	–0.18
C38H59N8O8	dw+H_2	755.44504	755.44508	0.05
C34H52N9O11	txy	762.37808	762.37856	0.63
C33H55N10O11	r+H	767.40463	767.40455	–0.10
C36H59N10O9	mpz+H or uvz+H	775.44610	775.44625	0.19
▲C34H55N10O11	ty+H_2	779.40463	779.40469	0.08
C37H61N10O9	pqg+H	789.46175	789.46174	–0.01
C37H60N9O10	pqg	790.44577	790.44541	–0.46
C35H57N10O11	t+H	793.42028	793.42044	0.20
C36H57N10O11	gA+H_2	805.42028	805.42052	0.30
C39H65N10O9	gB or gD	817.49305	817.49290	–0.18
C38H61N10O11	z+H	833.45185	833.45175	-0.12
C40H62N9O11	gx	844.45633	844.45644	0.13
C43H68N9O9	pE+H_2	854.51345	854.51358	0.15
▲C40H65N10O11	g+H	861.48288	861.48290	0.02
C44H68N9O9	ju	866.51345	866.51360	0.17
C44H67N10O9	lp-H_2	879.50870	879.50891	0.24
C42H69N10O12	F+H	905.50909	905.50902	–0.08
C46H67N7O12	Q	909.48422	909.48332	–0.99
C45H69N10O10	pG	909.51926	909.51947	0.23
C47H73N10O9	iB+H_2 or iD+H_2	921.55565	921.55541	–0.26
C46H70N9O11	RJ-H_2	924.51893	924.51895	0.02
C47H73N10O10	mp or uv	937.55057	937.55075	0.19
C48H70N9O11	ix	948.51893	948.51896	0.03
C48H75N10O10	B+H or D+H	951.56622	951.56645	0.24
C46H69N10O12	L+H	953.50909	953.50894	–0.16
C48H73N8O12	N+H	953.53425	953.53460	0.37
C48H73N10O11	i+H	965.54548	965.54551	0.03
C48H73N10O12	y+H	981.54039	981.54028	–0.11
▲C49H75N10O12	M+H	995.55604	995.55607	0.03
			Std. Dev.	0.26

applied CryoSpray ionization with a nebulizing gas temperature of –20°C, which enabled them to detect the MC–metal complexes [32]. In our experiments, the MC-LR standard was incubated individually with both Fe(II) and Fe(III) salt solutions, respectively, and directly applied to ESI without special consideration of the weak interactions. Interestingly, the observed metal binding was fairly stable under normal ESI conditions (nebulizing gas temperature at 200°C); strong signals were detected for doubly charged species (Figure 4) in both Fe(II) and Fe(III) incubations. Existing studies have reported different results for the Fe charge state within the MC–metal complex. Saito et al. only observed the MC-Fe(II) complex in the gas phase using a 9.4 T FTICR-MS instrument [32], whereas Klein et al. pointed out that the MC-Fe(III) complex should be more stable in the liquid phase, which the authors confirmed by electrochemistry experiments [52]. From our data, we initially also concluded only formation of the Fe(II) complex, but a closer look at the spectrum revealed that the isotope pattern of the doubly charged species did not match its theoretical simulation (Figure 4). Therefore, these species were isolated and re-analyzed using the narrowband mode in FTICR [54]. The high resolution data revealed that the doubly charged species was in fact a combination of patterns of $[M-H+Fe(III)]^{2+}$ and $[M+Fe(II)]^{2+}$ ions. Interestingly, $[M-H+Fe(III)]^{2+}$ and $[M+Fe(II)]^{2+}$ ions were always formed, even from the

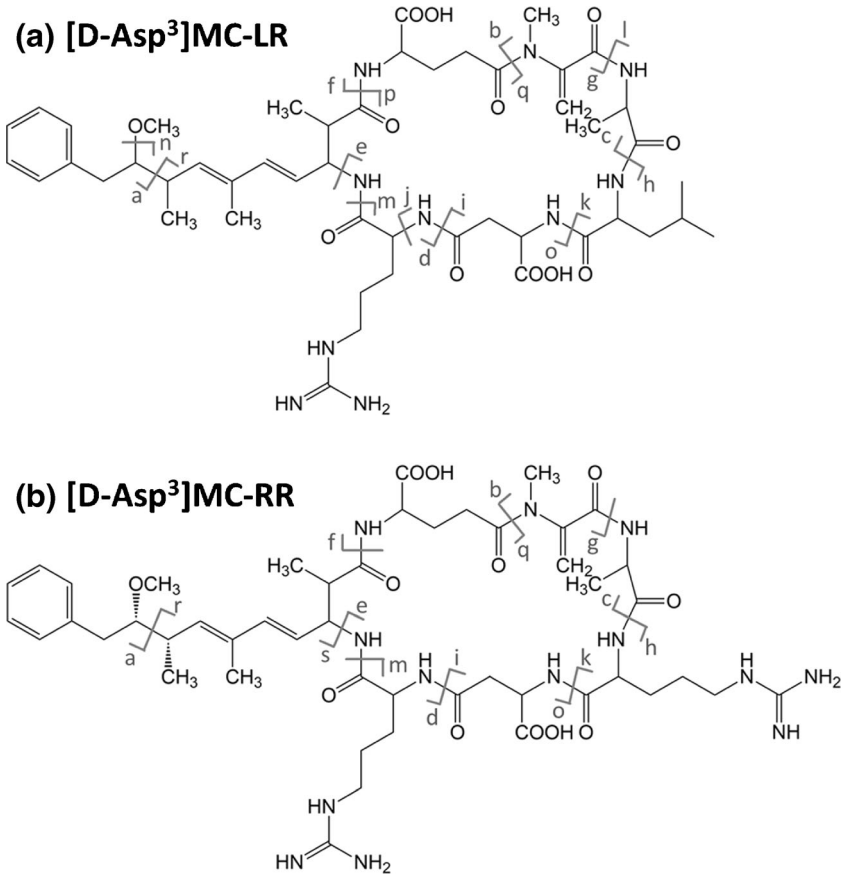

Figure 3. Illustration of the fragment assignments in CID mass spectra of doubly-charged [D-Asp^3]MC-LR (**a**) and [D-Asp^3]MC-RR (**b**). The full peak list is available in Tables S3 and S4 of the Supplementary Material

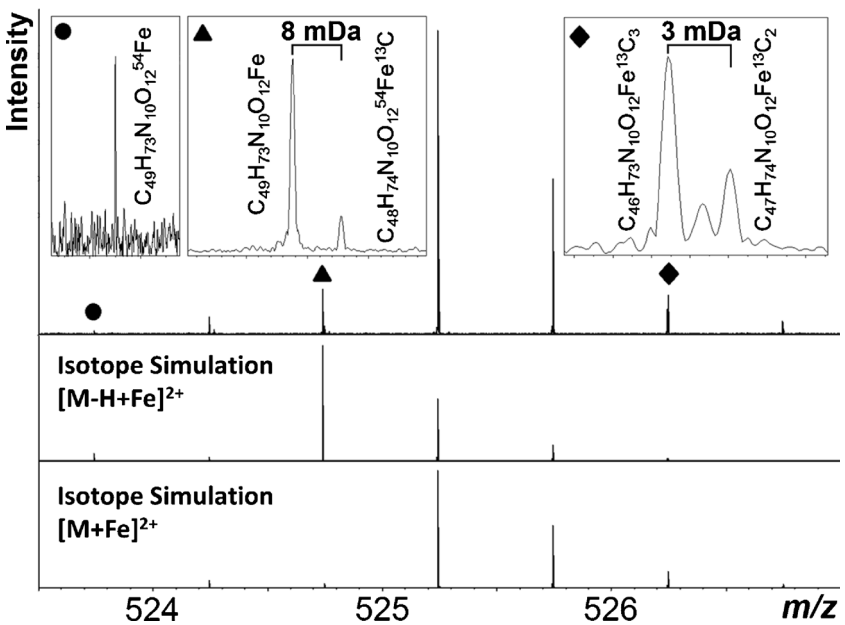

Figure 4. Spectrum of the MC-LR and Fe(II) complex, $[M-H+Fe(III)]^{2+}$ and $[M+Fe(II)]^{2+}$ ions, with the simulation of their isotope patterns. Note: the spectrum was recorded in narrowband mode (transient length >5 s) to achieve an average resolving power >600,000

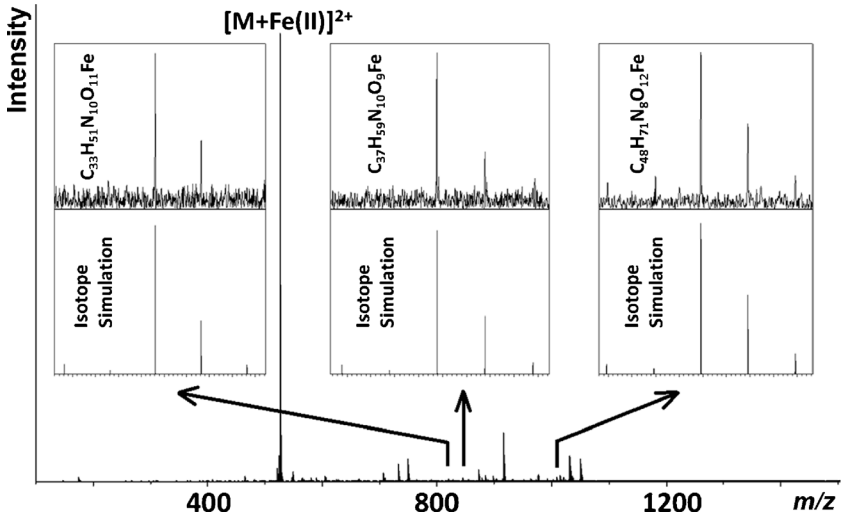

Figure 5. ECD spectrum of doubly-charged MC-LR and Fe complex ($[M+Fe(II)]^{2+}$ and $[M-H+Fe(III)]^{2+}$). The magnified insets demonstrate diagnostic fragment ions to locate the metal binding site

individual Fe(III) and Fe(III) incubations with the microcystin, with the $[M+Fe(II)]^{2+}$ species dominating over the Fe(III) species by ~7-fold. This observation suggests that oxidation/reduction reactions of Fe occurred in our experiment, likely during the ESI process [55]. Furthermore, the data indicate that both Fe(II) and Fe(III) can bind to MC-LR, and that the $[M+Fe(II)]^{2+}$ ion is more stable than $[M-H+Fe(III)]^{2+}$ in the gas phase, which might be the reason why Saito et al. did not observe the MC–Fe(III) complex [32]. To compare this binding behavior with other metals, MC-LR standard was also incubated with Mg(II) salt solution and analysed by FTICR-MS. As Mg cannot form a 3^+ charge state, the spectrum consequently only exhibited the $[M+Mg(II)]^{2+}$ species (see Supplementary Material).

Identifying the Metal Binding Sites of Microcystins LR and RR

Although MC-LR consists of only seven amino acids, it has several functional groups available for metal binding, such as ammonium (Arg), methoxy (Adda), and two carboxylic acid groups (Glu, MeAsp) [51]. Because metal coordination is much weaker than the bond energy of an amide bond, metal–MC bonds will dissociate before peptide backbone cleavage. Therefore, vibrational excitation MS/MS techniques such as low energy CID have usually failed to identify the metal binding sites of proteins [56, 57]. Consequently, the metal coordination sites of MCs have never been precisely located. Here, ECD was applied to study the Fe complex of MC-LR; Fe has a very distinctive isotope pattern compared with other common metals, which aided the rapid selection and assignment in the spectra.

ECD analysis of the cyclic peptide generated rich fragmentation with low peak intensities, thus requiring significant manual efforts to interpret the data as compared to CID. Fortunately, as shown above, ECD of MCs gave extensive side-chain fragmentation; these product ions could, therefore, be used as diagnostic peaks and greatly facilitated the data interpretation. Figure 5 illustrates the discovery of the metal binding site of MC-LR, which was located based on only three signature ions from side chain losses (note: labeling of fragments is explained in Figure 2d). First, the fragment "r" ($C_{33}H_{51}N_{10}O_{11}Fe^+$) corresponding to Adda, and the fragment "N" ($C_{48}H_{71}N_8O_{12}Fe^+$) corresponding to Arg, demonstrate that these two amino acids are not involved in the metal binding process. Consequently, the possible remaining binding sites are down to Glu and MeAsp. The observation of fragment "pqg" ($C_{37}H_{59}N_{10}O_9Fe^+$) finally confirmed that Fe was bound to MeAsp because cleavages at bond "p" and "q" caused the loss of the [COOH-CH-CH2] group, which is only possible to happen in Glu. The same experiment was then performed on MC-RR and the same diagnostic fragments were observed. Therefore, the primary Fe binding site for MCs was identified as MeAsp. Of course, this binding site assignment refers to the gas-phase and solution-phase behavior may differ, in particular considering different charge states of Fe in the gas phase [32] versus solution [52].

Conclusions

Nowadays, high performance mass spectrometry instruments such as FTICR-MS are increasingly applied to the analysis of natural products. This work has combined CID and ECD as fragmentation techniques to study microcystin variants expressed from a cyanobacterial strain, which was isolated from the Salto Grande Reservoir in Sao Paulo State in Brazil. The conventional CID technique showed its specificity for cleaving the amide bonds of the cyclic peptide, resulting in very simple MS/MS spectra with intensive fragment ion currents. This is an effective way to quickly confirm known MC compounds in environmental samples

for routine research applications or identify structurally related MC variants. The ECD method generated more extensive fragmentation levels, with unique ions from side chain losses, and provided complementary MS/MS data to CID. Therefore, this technique could be readily applied to more elaborate studies; for example, to study the biological mechanisms and intermediates of these toxins in cyanobacterial cells as well as biochemical mechanisms in the poisoned target organisms.

Acknowledgments

The authors thank Ernani Pinto (University of São Paulo, Brazil) for providing the MC-producing strain LTPNA 02, and Reiner Wintringer and Tobias Dier (Saarland University Saarbrücken) for technical support. S.B. is grateful for postdoctoral support through the Brazil Science without Borders program (Conselho Nacional de Desenvolvimento Científico e Tecnológico [CNPq], #201609/2012-6). D.A.V. acknowledges research support by the Alfried Krupp von Bohlen und Halbach-Stiftung.

References

1. van Apeldoorn, M.E., van Egmond, H.P., Speijers, G.J.A., Bakker, G.J.I.: Toxins of cyanobacteria. Mol Nutr Food Res **51**(1), 7–60 (2007)
2. Welker, M., Von Döhren, H.: Cyanobacterial peptides—nature'' own combinatorial biosynthesis. FEMS Microbiol Rev **30**(4), 530–563 (2006)
3. Zurawell, R.W., Chen, H., Burke, J.M., Prepas, E.E.: Hepatotoxic cyanobacteria: a review of the biological importance of microcystins in freshwater environments. J. Toxicol. Environ. Health, Part B **8**(1), 1–37 (2005)
4. Wood, S.A., Mountfort, D., Selwood, A.I., Holland, P.T., Puddick, J., Cary, S.C.: Widespread distribution and identification of eight novel microcystins in antarctic cyanobacterial mats. Appl Environ Microbiol **74**(23), 7243–7251 (2008)
5. Jochimsen, E.M., Carmichael, W.W., An, J., Cardo, D.M., Cookson, S.T., Holmes, C.E.M., Antunes, M.B., de Melo Filho, D.A., Lyra, T.M., Barreto, V.S.T., Azevedo, S.M.F.O., Jarvis, W.R.: Liver failure and death after exposure to microcystins at a hemodialysis center in Brazil. N Engl J Med **338**(13), 873–878 (1998)
6. Bartram, J., Chorus, I.: Toxic Cyanobacteria in Water: A Guide to their Public Health Consequences, Monitoring and Management. Taylor & Francis: p. 41 (2002)
7. del Campo, F.F., Ouahid, Y.: Identification of microcystins from three collection strains of *Microcystis aeruginosa*. Environ Pollut **158**(9), 2906–2914 (2010)
8. Bortoli, S., Volmer, D.: Account: characterization and identification of microcystins by mass spectrometry. Eur. J. Mass Spectrom **20**(1), 1–19 (2014)
9. Sano, T., Beattie, K.A., Codd, G.A., Kaya, K.: Two (Z)-dehydrobutyrine-containing microcystins from a hepatotoxic bloom of *Oscillatoria agardhii* from Soulseat Loch. . J. Nat. Prod. Scotland **61**(6), 851–853 (1998)
10. Rinehart, K., Namikoshi, M., Choi, B.: Structure and biosynthesis of toxins from blue-green algae (cyanobacteria). J Appl Phycol **6**(2), 159–176 (1994)
11. Carmichael, W.W.: Cyanobacteria secondary metabolites—the cyanotoxins. J Appl Bacteriol **72**(6), 445–459 (1992)
12. Goldberg, J., Huang, H.B., Kwon, Y.G., Greengard, P., Nairn, A.C.: Kuriyan, J: Three-dimensional structure of the catalytic subunit of protein serine/threonine phosphatase - 1. Nature **376**(6543), 745–753 (1995)
13. Pereira, S.R., Vasconcelos, V.M., Antunes, A.: Computational study of the covalent bonding of microcystins to cysteine residues—a reaction involved in the inhibition of the PPP family of protein phosphatases. FEBS J **280**(2), 674–680 (2013)
14. Dittmann, E., Wiegand, C.: Cyanobacterial toxins—occurrence, biosynthesis, and impact on human affairs. Mol Nutr Food Res **50**(1), 7–17 (2006)
15. Krishnamurthy, T., Carmichael, W.W., Sarver, E.W.: Toxic peptides from freshwater cyanobacteria (blue-green algae). I. Isolation, purification, and characterization of peptides from *Microcystis aeruginosa* and *Anabaena flos-aquae*. Toxicon **24**(9), 865–873 (1986)
16. Namikoshi, M., Rinehart, K.L., Sakai, R., Stotts, R.R., Dahlem, A.M., Beasley, V.R., Carmichael, W.W., Evans, W.R.: Identification of 12 hepatotoxins from a Homer Lake bloom of the cyanobacteria *Microcystis aeruginosa*, *Microcystis viridis*, and *Microcystis wesenbergii*: nine new microcystins. J Org Chem **57**(3), 866–872 (1992)
17. Lukač, M., Aegerter, R.: Influence of trace metals on growth and toxin production of *Microcystis aeruginosa*. Toxicon **31**(3), 293–305 (1993)
18. Utkilen, H., Gjølme, N.: Iron-stimulated toxin production in *Microcystis aeruginosa*. Appl Environ Microbiol **61**(2), 797–800 (1995)
19. Horne, A.J., Goldman, C.R., Goldman, C.R.L.: Limnology, 2nd ed. Horne, A.J., Goldman. C.R., Eds., McGraw-Hill: New York; London (1994)
20. Botes, D.P., Tuinman, A.A., Wessels, P.L., Viljoen, C.C., Kruger, H., Williams, D.H., Santikarn, S., Smith, R.J., Hammond, S.J.: The structure of cyanoginosin-LA, a cyclic heptapeptide toxin from the cyanobacterium *Microcystis aeruginosa*. J Chem Soc Perkin Trans **1**, 2311–2318 (1984)
21. Rinehart, K.L., Harada, K., Namikoshi, M., Chen, C., Harvis, C.A., Munro, M.H.G., Blunt, J.W., Mulligan, P.E., Beasley, V.R., Dahlem, A. M., Carmichael, W.W.: *Nodularin*, *microcystin*, and the configuration of Adda. J Am Chem Soc **110**(25), 8557–8558 (1988)
22. Luukkainen, R., Namikoshi, M., Sivonen, K., Rinehart, K.L., Niemelä, S.I.: Isolation and identification of 12 microcystins from four strains and two bloom samples of *Microcystis* spp.: structure of a new hepatotoxin. Toxicon **32**(1), 133–139 (1994)
23. Poon, G.K., Griggs, L.J., Edwards, C., Beattie, K.A., Codd, G.A.: Liquid chromatography-electrospray ionization-mass spectrometry of cyanobacterial toxins. J Chromatogr A **628**(2), 215–233 (1993)
24. Bateman, K.P., Thibault, P., Douglas, D.J., White, R.L.: Mass spectral analyses of microcystins from toxic cyanobacteria using on-line chromatographic and electrophoretic separations. J Chromatogr A **712**(1), 253–268 (1995)
25. Namikoshi, M., Yuan, M., Sivonen, K., Carmichael, W.W., Rinehart, K.L., Rouhiainen, L., Sun, F., Brittain, S., Otsuki, A.: Seven new microcystins possessing two l-glutamic acid units, isolated from *Anabaena* sp. strain 186. Chem Res Toxicol **11**(2), 143–149 (1998)
26. Kubwabo, C., Vais, N., Benoit, F.M.: Characterization of microcystins using in-source collision-induced dissociation. Rapid Commun Mass Spectrom **19**(5), 597–604 (2005)
27. Frias, H.V., Mendes, M.A., Cardozo, K.H.M., Carvalho, V.M., Tomazela, D., Colepicolo, P., Pinto, E.: Use of electrospray tandem mass spectrometry for identification of microcystins during a cyanobacterial bloom event. Biochem Biophys Res Commun **344**(3), 741–746 (2006)
28. Dörr, F.A., Oliveira-Silva, D., Lopes, N.P., Iglesias, J., Volmer, D.A., Pinto, E.: Dissociation of deprotonated microcystin variants by collision-induced dissociation following electrospray ionization. Rapid Commun Mass Spectrom **25**(14), 1981–1992 (2011)
29. Diehnelt, C.W., Dugan, N.R., Peterman, S.M., Budde, W.L.: Identification of microcystin toxins from a strain of *Microcystis aeruginosa* by liquid chromatography introduction into a hybrid linear ion trap-Fourier transform ion cyclotron resonance mass spectrometer. Anal Chem **78**(2), 501–512 (2005)
30. Sleno, L., Volmer, D.A.: Ion activation methods for tandem mass spectrometry. J Mass Spectrom **39**(10), 1091–1112 (2004)
31. Mayumi, T., Kato, H., Imanishi, S., Kawasaki, Y., Hasegawa, M., Harada, K.: Structural characterization of microcystins by LC/MS/MS under ion trap conditions. J Antibiot **59**(11), 710–719 (2006)
32. Saito, K., Sei, Y., Miki, S., Yamaguchi, K.: Detection of microcystin–metal complexes by using cryospray ionization-Fourier transform ion cyclotron resonance mass spectrometry. Toxicon **51**(8), 1496–1498 (2008)
33. Zubarev, R., Haselmann, K., Budnik, B., Kjeldsen, F., Jensen, F.: Account: towards an understanding of the mechanism of electron-

capture dissociation: a historical perspective and modern ideas. Eur. J. Mass Spectrom **8**(5), 337–349 (2002)
34. Zubarev, R.A., Kelleher, N.L., McLafferty, F.W.: Electron capture dissociation of multiply charged protein cations—a nonergodic process. J Am Chem Soc **120**(13), 3265–3266 (1998)
35. Leymarie, N., Costello, C.E., O'Connor, P.B.: Electron capture dissociation initiates a free radical reaction cascade. J Am Chem Soc **125**(29), 8949–8958 (2003)
36. Ueberheide, B.M., Fenyö, D., Alewood, P.F., Chait, B.T.: Rapid sensitive analysis of cysteine rich peptide venom components. Proc Natl Acad Sci **106**(17), 6910–6915 (2009)
37. Samgina, T.Y., Artemenko, K.A., Gorshkov, V.A., Ogourtsov, S.V., Zubarev, R.A., Lebedev, A.T.: Mass spectrometric study of peptides secreted by the skin glands of the brown frog *Rana arvalis* from the Moscow region. Rapid Commun Mass Spectrom **23**(9), 1241–1248 (2009)
38. Gorham, P.R., McLachlan, J., Hammer, U.T., Kim, W.K.: Isolation and culture of toxic strains of *Anabaena flos-aquae* (Lyngb.) de Bréb. Verein. Limnol **15**(8), 796–804 (1964)
39. Carmichael, W.W., Gorham, P.R.: an improved method for obtaining axenic clones of planktonic blue-green algae 1,2. J Phycol **10**(2), 238–240 (1974)
40. Qi, Y., O'Connor, P. B.: Data processing in Fourier transform ion cyclotron resonance mass spectrometry. Mass Spectrom. (2014) doi:10.1002/mas.21414
41. Zubarev, R.A., Horn, D.M., Fridriksson, E.K., Kelleher, N.L., Kruger, N.A., Lewis, M.A., Carpenter, B.K., McLafferty, F.W.: Electron capture dissociation for structural characterization of multiply charged protein cations. Anal Chem **72**(3), 563–573 (2000)
42. O'Connor, P.B., Lin, C., Cournoyer, J.J., Pittman, J.L., Belyayev, M., Budnik, B.A.: Long-lived electron capture dissociation product ions experience radical migration via hydrogen abstraction. J Am Soc Mass Spectrom **17**(4), 576–585 (2006)
43. Ferranti, P., Fabbrocino, S., Nasi, A., Caira, S., Bruno, M., Serpe, L., Gallo, P.: Liquid chromatography coupled to quadruple time-of-flight tandem mass spectrometry for microcystin analysis in freshwaters: method performances and characterisation of a novel variant of microcystin-RR. Rapid Commun Mass Spectrom **23**(9), 1328–1336 (2009)
44. Wills, R.H., Tosin, M., O'Connor, P.B.: Structural characterization of polyketides using high mass accuracy tandem mass spectrometry. Anal Chem **84**(20), 8863–8870 (2012)
45. Mosely, J.A., Smith, M.J.P., Prakash, A.S., Sims, M., Bristow, A.W.T.: Electron-induced dissociation of singly charged organic cations as a tool for structural characterization of pharmaceutical type molecules. Anal Chem **83**(11), 4068–4075 (2011)
46. Kaczorowska, M., Cooper, H.: Electron induced dissociation: a mass spectrometry technique for the structural analysis of trinuclear oxo-centred carboxylate-bridged iron complexes. J Am Soc Mass Spectrom **21**(8), 1398–1403 (2010)
47. Krüger, T., Christian, B., Luckas, B.: Development of an analytical method for the unambiguous structure elucidation of cyclic peptides with special appliance for hepatotoxic desmethylated microcystins. Toxicon **54**(3), 302–312 (2009)
48. Diehnelt, C.W., Peterman, S.M., Budde, W.L.: Liquid chromatography-tandem mass spectrometry and accurate *m*/*z* measurements of cyclic peptide cyanobacteria toxins. TrAC Trends Anal Chem **24**(7), 622–634 (2005)
49. Zweigenbaum, J.A., Henion, J.D., Beattie, K.A., Codd, G.A., Poon, G.K.: Direct analysis of microcystins by microbore liquid chromatography electrospray ionization ion-trap tandem mass spectrometry. J Pharm Biomed Anal **23**(4), 723–733 (2000)
50. Watanabe, M.F., Tsuji, K., Watanabe, Y., Harada, K., Suzuki, M.: Release of heptapeptide toxin (microcystin) during the decomposition process of Microcystis aeruginosa. Nat Toxins **1**(1), 48–53 (1992)
51. Humble, A.V., Gadd, G.M., Codd, G.A.: Binding of copper and zinc to three cyanobacterial microcystins quantified by differential pulse polarography. Water Res **31**(7), 1679–1686 (1997)
52. Klein, A.R., Baldwin, D.S., Silvester, E.: Proton and iron binding by the cyanobacterial toxin microcystin-LR. Environ Sci Technol **47**(10), 5178–5184 (2013)
53. Yan, F., Ozsoz, M., Sadik, O.A.: Electrochemical and conformational studies of microcystin-LR. Anal Chim Acta **409**(1/2), 247–255 (2000)
54. Amster, I.J.: Fourier transform mass spectrometry. J Mass Spectrom **31**(12), 1325–1337 (1996)
55. Rohner, T.C., Lion, N., Girault, H.H.: Electrochemical and theoretical aspects of electrospray ionisation. Phys Chem Chem Phys **6**(12), 3056–3068 (2004)
56. Qi, Y., Liu, Z., Li, H., Sadler, P.J., O'Connor, P.B.: Mapping the protein-binding sites for novel iridium(III) anticancer complexes using electron capture dissociation. Rapid Commun Mass Spectrom **27**(17), 2028–2032 (2013)
57. Li, H., Lin, T.-Y., Van Orden, S.L., Zhao, Y., Barrow, M.P., Pizarro, A.M., Qi, Y., Sadler, P.J., O'Connor, P.B.: Use of top-down and bottom-up Fourier transform ion cyclotron resonance mass spectrometry for mapping calmodulin sites modified by platinum anticancer drugs. Anal Chem **83**(24), 9507–9515 (2011)